

**Unusual Time-Dependent Phenomena in Taylor-Couette Flow at Moderately Low Reynolds Numbers**

T. Mullin

*Clarendon Laboratory, University of Oxford, Oxford OX1 3PU, United Kingdom*

K. A. Cliffe

*Theoretical Physics Division, Harwell Laboratory, Oxon OX11 0RA, United Kingdom*

and

G. Pfister

*University of Kiel, Kiel, West Germany*

(Received 16 December 1986)

The results of an experimental and numerical investigation into a new mechanism for the onset of time dependence in Taylor-Couette flow are presented. The interaction between a symmetry-breaking bifurcation and a fold point gives rise to Hopf bifurcation. The resulting time-dependent flows may be either periodic or irregular.

PACS numbers: 47.20.-k, 47.15.-x, 47.30.+s

The Taylor-Couette experiment concerns the flow generated between concentric cylinders when the inner one rotates and the outer one is held stationary.<sup>1</sup> As the speed of the inner cylinder is raised, steady cellular flows which appear initially are followed in turn by time-periodic and quasiperiodic motions. At even higher values of the Reynolds number  $R$  (the nondimensional speed of the inner cylinder), irregular motions occur which are chaotic in the temporal sense,<sup>2</sup> although there usually remains some definite spatial structure in the flow.

It is known that both the steady and time-dependent states are nonunique,<sup>3-5</sup> and the cell-selection process in the steady regime is reviewed by Mullin and Cliffe.<sup>6</sup> The main question addressed is how the uniquely defined *primary* cellular state, formed by continuous increase in  $R$  from small values, changes as the length of the fluid column is varied. The exchange proceeds via the interaction with a disconnected *secondary* branch which becomes primary when the length is changed. Our studies to date have been restricted to comparatively small values of the aspect ratio  $\Gamma$  ( $=l/d$ , where  $l$  is the length and  $d$  is the gap width); because the multiplicity of the solution set is thereby limited, the delicate exchange process is made more distinctive.

Recent numerical work<sup>7</sup> has shown that symmetry-breaking bifurcations are important in the selection process. In order to obtain agreement between the experimental and numerical results for the 4/6-cell interaction, allowance must be made for symmetry breaking by steady flows that do not preserve the up-down symmetry about the midplane of the fluid-filled annulus. The path of symmetry-breaking bifurcation points, which lies on the surface of symmetric solutions, can move from the stable to the unstable part of the surface as the aspect ratio is varied. This process gives rise to a singular point

with geometric and algebraic multiplicity two, where the symmetry-breaking bifurcation point coincides with the limit point. We report experimental and numerical results obtained close to such a double-singular point, which exhibit interesting dynamical behavior.

The apparatus consists of a machined inner cylinder of radius  $r_1 = 12.5 \pm 0.01$  mm which is located concentrically in a precision-bore outer cylinder of radius  $r_2 = 25.0 \pm 0.01$  mm, giving a radius ratio  $\eta = r_1/r_2 = 0.5$ . The inner cylinder is rotated by a dc phase-locked loop motor which has an accuracy of better than 0.1%. The cylinders are contained within a square box through which temperature-controlled fluid is circulated, so that the temperature of the working fluid is held constant to within 0.01 K. The overall aim is to control the value of  $R$  to better than 0.1%, which is essential for the study of the time-dependent phenomena in question. (Note that  $R = \omega r_1 d / \nu$ , where  $\omega$  is the angular frequency of the inner cylinder,  $d = r_2 - r_1$ , and  $\nu$  is the kinematic viscosity.)

The radial velocity component is measured with a laser-Doppler velocimeter operating in the forward-scatter mode. In order to obtain good signal quality the working fluid, silicone oil with a viscosity  $\nu = 34.22$  cS, is seeded with latex spheres of diameter  $2 \mu\text{m}$ . The signal is processed by a phase-locked loop tracker which gives a voltage output proportional to the velocity. Steady velocity profiles can then be measured by movement of the entire apparatus on a traversing lift. In addition, time-dependent modes may be studied at preselected positions and the velocity-time signature processed by software<sup>8</sup> to produce the autocorrelation function, which may be Fourier transformed to give the power spectrum.

The length of the fluid column is determined by two nonrotating end plates. The position of the top plate may be accurately adjusted by use of an external cali-

brated micrometer. The length measurement may be cross-checked by our noting the positions at which the laser beams intersect the end plates when a traverse is made.

In this investigation we have concentrated on the four-cell state as a secondary mode. The loci of critical points are presented in Fig. 1 in terms of  $\Gamma$  and  $R$ . The solid lines are obtained from computation of the Navier-Stokes equations with appropriate boundary conditions by numerical bifurcation techniques<sup>7,9</sup> and the points are determined experimentally. The line  $AB$  is the locus of limit points of the symmetric solution and has not been investigated experimentally in this study, although a detailed experimental and numerical investigation has been performed for another radius ratio.<sup>10</sup>  $AC$  is the locus of symmetry-breaking bifurcation points which lie on the unstable part of the symmetric solution surface and can therefore not be observed experimentally. The point  $A$  is a double singular point where the limit and symmetry-breaking bifurcation point coincide.

Higher-order bifurcations of this type are known to be accompanied by Hopf bifurcations.<sup>11,12</sup> The mechanism for the occurrence of the Hopf bifurcations is illustrated in Fig. 2. In Fig. 2(a), the aspect ratio is such that the symmetry-breaking bifurcation lies on the stable part of

the solution surface. Thus, by continuity, the solution branch emerging at the bifurcation point will be stable too. In an experiment one would observe the development of an asymmetric state as  $R$  is reduced through the bifurcation point. The bifurcation will of course be disconnected by the presence of imperfections in the apparatus, but a sharp change in symmetry is found.<sup>10</sup> (The magnitude of the asymmetry is very small and great care is needed for its reliable detection, but as will be seen below the consequences of its presence are far reaching.)

Figure 2(b) shows that as the aspect ratio is changed the symmetry-breaking bifurcation point moves onto the unstable part of the symmetric-solution surface. Continuity indicates that on the asymmetric branches, close to the bifurcation point, the linearized operator has two eigenvalues in the unstable half of the complex plane. (These eigenvalues are continuously connected to those on the symmetric-solution surface whose corresponding eigenvectors are symmetric and antisymmetric, respectively.) However, continuity arguments also indicate that sufficiently far from the bifurcation the branches should be stable since a continuous change in  $\Gamma$  takes us from Fig. 2(b) to Fig. 2(a). [Note that the reverse situation can occur where the branches in 2(b) are unstable

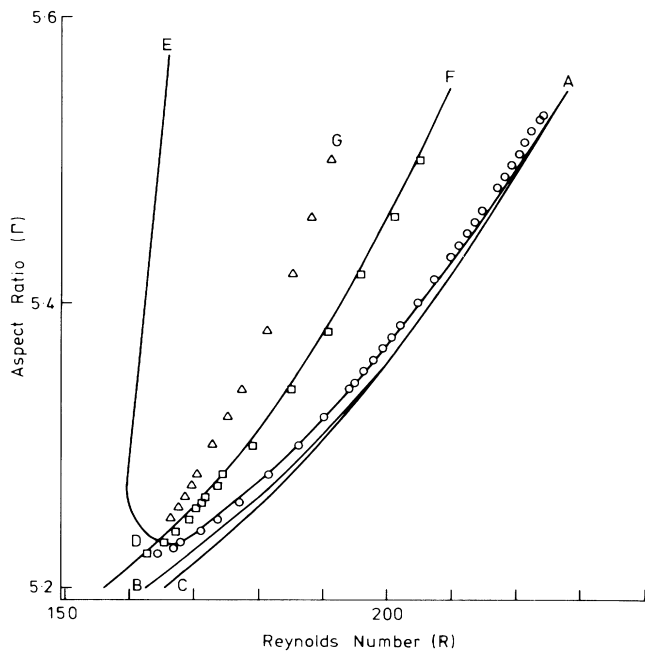


FIG. 1. Comparison between the experimental and numerical results for the bifurcation set.  $AB$  is the path of supercritical fold points.  $AC$  is the path of subcritical symmetry-breaking bifurcation points.  $ADE$  is the line of axisymmetric Hopf bifurcation points.  $DF$  is the line of subcritical Hopf bifurcation points giving rise to the tilt wave.  $DG$  are the measured points for the onset of axisymmetric modulation of the tilt wave.

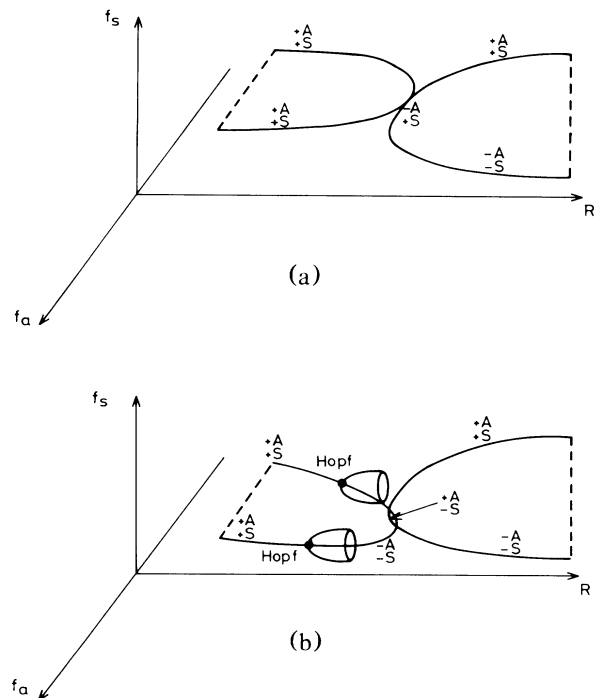


FIG. 2. Schematic bifurcation diagrams for an aspect ratio (a) greater than that at  $A$  in Fig. 1 and (b) less than that at  $A$  and greater than that at  $D$  in Fig. 1.  $f_s$  measures the symmetric component of the solution and  $f_a$  the antisymmetric component. The symbols  $+A$ ,  $+S$ ,  $(-A, -S)$  indicate stability (instability) to asymmetric and symmetric perturbations.

and those in 2(a) are initially stable and then become unstable.] The simplest way to account for the situation is as follows: As  $R$  is decreased along the asymmetric branch in Fig. 2(b) the two real eigenvalues first coalesce and form a complex-conjugate pair which then crosses the imaginary axis, thereby ending up in the stable half plane. This mechanism leads to the presence of a Hopf bifurcation and thus to periodic orbits. A path of Hopf bifurcations on the asymmetric surface emanates from the double singular point. Further, the frequency of the periodic orbit should approach zero at the double singular point and will be small in general.

The line  $ADE$  in Fig. 1 originates at the double singular point  $A$  and is the locus of Hopf bifurcations into an axisymmetric oscillation. Oscillations which have similar spatial characteristics to these have recently been reported,<sup>13</sup> but it is not clear if they are of the same type. The numerical results give the location of the Hopf points and indicate whether the bifurcation is subcritical or supercritical, but the program cannot yet compute the periodic orbits, so that we cannot follow the bifurcating branch. The Hopf bifurcation was found, numerically, to be supercritical along  $AD$  and subcritical along  $DE$ , so that the axisymmetric oscillation exists for parameter values outside the region enclosed by  $ADE$ . The oscillation to the right of  $AD$  was confirmed to be axisymmetric in the experiment by our splitting the laser system and using two detectors to determine the phase relationship around the cylindrical gap. Each bifurcation point in the experiment was determined at a fixed value of  $\Gamma$  by our varying  $R$ . The variations were such that equilibrium operating conditions were always maintained.

The experimental measurements of the axisymmetric oscillation were extremely difficult to perform. These oscillations arise at supercritical bifurcations on the asymmetric branches which are bounded by unstable sections at either end. Therefore, these branches must either be located by jumping to them by trial and error or be reached via larger aspect ratios where they are continuously connected to the stable part of the fold. The second method is not efficient as the steady asymmetric mode is very sensitive to perturbations introduced by movement of the end plates. Therefore the method of trial and error was adopted.

The oscillations arising at the Hopf bifurcation were found to be extremely sensitive to variations in  $R$ . A typical statistic is that a 0.26% change in  $R$  gave a 13% change in period and approximately doubled the amplitude. The wave form rapidly changed from sinusoidal very close to the bifurcation point to a large-amplitude triangular shape as  $R$  was increased. When  $R$  was further increased to around 1% above the bifurcation point, the amplitude became so large that the mode collapsed to the six-cell symmetric state which is the primary flow.

The periods of the axisymmetric oscillation were long compared with the normal wavy flows found in the

Taylor-Couette system. With the fluid used here, they were in the range 12–70 s with the longer periods nearer point  $A$ . A comparison between the numerical and experimental nondimensionalized frequencies is given in Fig. 3. The scatter in the data is due to the extreme sensitivity of the frequency to changes in  $R$  mentioned above. At aspect ratio 5.512 the oscillation observed in the experiment is initially regular but becomes irregular upon increase of  $R$ . The irregularity takes the form of occasional bursts in the velocity-time trace superposed on the regular oscillation. The power spectrum (averaged over 16 h) for the irregular flows is presented in Fig. 4 where the dominant peak of the main wave can be seen together with a low-frequency broad-band component.

The line  $DF$  in Fig. 1 is the locus of Hopf bifurcation points into an azimuthal traveling wave with wave number 1. The bifurcation is subcritical, i.e., the onset of the wave occurs with decrease in  $R$ . This is the normal tilt wave such that there is a  $180^\circ$  phase difference on opposite sides of the annulus.

The line  $DG$  is the experimentally determined locus for the onset of axisymmetric modulation of the tilt wave and is found by further reduction in  $R$ . We believe that this arises as secondary bifurcation at the multiple bifurcation point  $D$ , where there is an exchange of stabilities between the two modes. Further reduction of  $R$  to a few

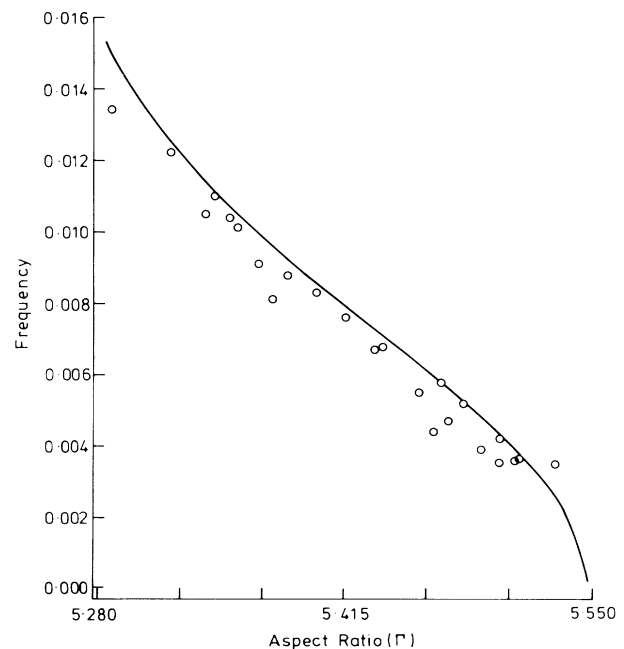


FIG. 3. Comparison between the experimental and numerical results for the nondimensional frequency of the axisymmetric wave as a function of  $\Gamma$ . The wave frequency has been nondimensionalized by division with the inner-cylinder frequency.

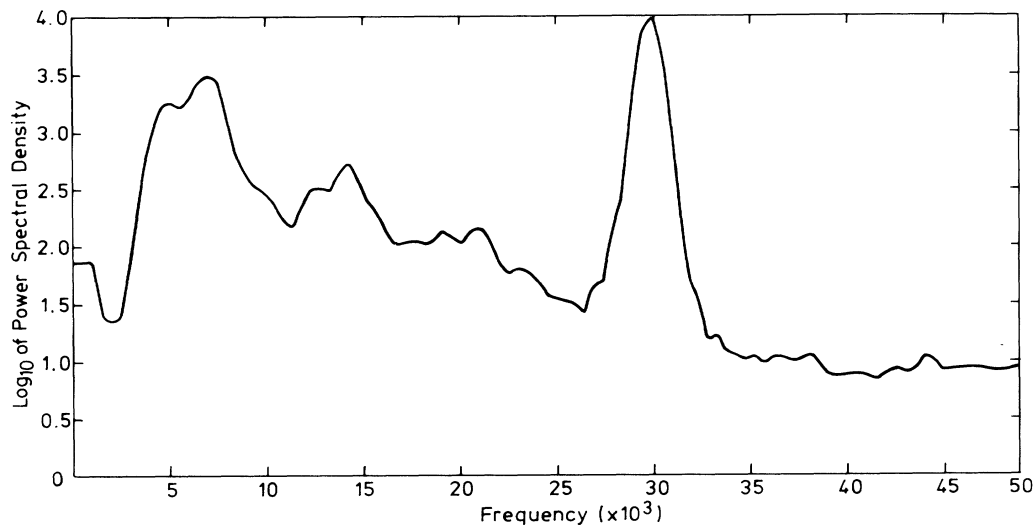


FIG. 4. Power spectrum of the radial component of velocity measured in the midplane in the chaotic regime, plotted on a logarithmic scale.

percent below  $DG$  causes the collapse of the time-dependent mode back to the primary six-cell state. The computed curve  $DE$  is the locus of subcritical bifurcation points to the axisymmetric oscillations, but it is not observable since the axisymmetric flow is unstable.

The numerical and experimental results indicate the presence of periodic orbits whose frequency tends to zero as the double singular point is approached. The detailed dynamical behavior could be studied by use of center-manifold theory and computation of the coefficients of the nonlinear terms numerically. This will be done in the future. However, we can infer from the symmetry in the problem that the equations will have the form

$$\begin{aligned} \dot{r} &= r(\epsilon + a_2 z + b_1 r^2 + b_2 z^2) \\ &\quad + \text{higher-order terms,} \\ \dot{z} &= \mu + a_3 r^2 + a_4 z^2 + b_3 r^2 + b_4 z^3 \\ &\quad + \text{higher-order terms,} \end{aligned} \quad (1)$$

where  $r$  and  $z$  are the amplitudes of the antisymmetric and symmetric modes, respectively, and  $\epsilon$  and  $\mu$  depend on  $R$  and  $\Gamma$ . This system has been studied by Guckenheimer,<sup>11</sup> who showed that its asymptotic behavior depends on the magnitude of the coefficients and that, for appropriate values, the behavior is similar to that observed here. It is also known that a periodic forcing of systems like Eq. (1) can lead to chaotic behavior. Thus the irregular motion observed in the experiment may be due to small imperfections producing a periodic forcing at the rotation frequency of the inner cylinder.

The authors are grateful to Professor T. B. Benjamin for many helpful discussions concerning this work. The research of one of us (T.M.) is supported by the Science and Engineering Research Council. Another of us

(K.A.C.) is supported by the Underlying Program of the United Kingdom Atomic Energy Authority and the Royal Society under the Royal Society/Science and Engineering Research Council Industrial Fellowship scheme. One of us (G.P.) is supported by Stiftung Volkswagenwerk.

<sup>1</sup>R. C. DiPrima and H. L. Swinney, in *Hydrodynamic Instabilities and the Transition to Turbulence*, edited by H. L. Swinney and J. P. Gollub (Springer-Verlag, Berlin, 1981).

<sup>2</sup>A. Brandstätter, J. Swift, H. L. Swinney, A. Wolf, J. D. Farmer, E. Jen, and J. P. Crutchfield, *Phys. Rev. Lett.* **51**, 1442 (1983).

<sup>3</sup>J. E. Burkhalter and E. L. Koschmieder, *Phys. Fluids* **17**, 1929 (1974).

<sup>4</sup>T. B. Benjamin and T. Mullin, *J. Fluid Mech.* **121**, 219 (1982).

<sup>5</sup>D. Coles, *J. Fluid Mech.* **21**, 385 (1965).

<sup>6</sup>T. Mullin and K. A. Cliffe, in *Nonlinear Phenomena and Chaos*, edited by S. Sarkar (Hilger, London, 1986).

<sup>7</sup>K. A. Cliffe, to be published.

<sup>8</sup>G. Pfister, U. Gerdtz, A. Lorenzen, and K. Schätzel, in *Photon Correlation Techniques*, edited by E. O. Schulz-DuBois, Springer Series in Optical Sciences Vol. 38 (Springer-Verlag, Berlin, 1983), p. 256.

<sup>9</sup>See *Numerical Methods in Bifurcation Theory*, edited by T. Küpper, H. D. Mittelmann, and H. Weber (Birkhäuser, Basel, 1984).

<sup>10</sup>K. A. Cliffe and T. Mullin, unpublished.

<sup>11</sup>J. Guckenheimer, in *Dynamical Systems and Turbulence, Warwick, 1980*, edited by D. A. Rand and L.-S. Young, Lecture Notes in Mathematics Vol. 898 (Springer-Verlag, Berlin, 1981).

<sup>12</sup>I. Rehberg and G. Ahlers, *Phys. Rev. Lett.* **55**, 500 (1985).

<sup>13</sup>L. Zhang and H. L. Swinney, *Phys. Rev. A* **31**, 1006 (1985).